JOURNAL OF PHYSICAL ORGANIC CHEMISTRY, VOL. 6, 29–43 (1993)

EFFECTS CONTROLLING THE CONFORMATIONAL SELECTIVITY AND ASSOCIATION PARAMETERS OF H-BONDED ASSEMBLIES BETWEEN DI- AND TRIAMINOTRIAZINES AND BEMEGRIDE

ITAMAR WILLNER,* JACQUELINE ROSENGAUS AND YOAV EICHEN
Institute of Chemistry, Hebrew University of Jerusalem, Jerusalem 91904, Israel

2,4,6-Tris(aminocyclohexyl)triazine (1) and 2,4-bis(aminocyclohexyl)-6-methoxytriazine (2) are present in solution in two and three equilibrating conformations, respectively. The activation barrier for interconversion of the conformers 1a ⇌ 1b is 14·55 ± 0·2 kcal mol^{-1} (1 kcal = 4·184 kJ) and the activation barrier for interconversion of the conformers 2a ⇌ 2b ⇌ 2c is 14·2 ± 0·2 kcal mol^{-1}. The conformational analyses of 1 and 2 were also followed by molecular mechanics calculations. Compounds 1 and 2 form H-bonded intermolecular complexes with bemegride (3). Association of 3 proceeds by selection of a specific conformation of 1 and 2, i.e. 1b and 2a, respectively. The association constants of 3–1b and 3–2a are to $K_a = 915$ and 450 l mol^{-1}, respectively. Molecular mechanics calculations for the H-bonded intermolecular assemblies support the experimental observations of the selective conformational association.

INTRODUCTION

Conformational selectivity plays an important role in the association of compounds to biomaterials.[1] Extensive research activity is directed towards the design of supramolecular host–guest assemblies originating from complementary H-bonded interactions.[2,3] Both experimental[4] and theoretical studies[5] have revealed the roles of structural features of the two molecular components on the stability of the resulting H-bonded intramolecular assembly. The characterization of such intramolecular interactions provides model systems for biological materials, e.g. DNA, and allows the design of intramolecular compositions of crystalline materials. In addition, such supramolecular assemblies allow their further development into catalytic moieties mimicking the functions of enzymes. Selective association of an energetically unfavoured guest conformation to a host molecule has recently been highlighted by Vincent *et al.*[6] In that study the terphthaloyl receptor was found to associate selectively with the *S-cis* rotamer of succinamide diacid, being the less favoured rotamer of the host compound.

Several recent studies have applied aminotriazines and diazines as building sites for the construction of multi-dimensional H-bonded networks.[7] Also, H-bonded assemblies utilizing diaminotriazine as a host molecule were recently characterized at a water–air interface.[8] In this paper we describe the conformational properties of 2,6-bis(aminocyclohexyl)-4-methoxytriazine (1) and 2,4,6-tris(aminocyclohexyl)triazine (2) and reveal the selective discrimination of specific conformations of this triazine compound in the formation of H-bonded assemblies. The experimental results are supported by molecular mechanics calculations.

EXPERIMENTAL

General. ^{1}H and ^{13}C NMR spectra were obtained on a Bruker AMX/400 instrument. All chemicals were purchased from Aldrich. Association constants were calculated using the Benesi–Hildebrand equation.[9] $CDCl_3$ was dried over calcium chloride and used as the solvent in all NMR studies.

2,4,-Bis(aminocyclohexyl)-6-chlorotriazine. 2,4-Bis (aminocyclohexyl)-6-chlorotriazine was prepared using the general procedure described by Thurston and coworkers.[10] A solution of 10 g (54·34 mmol) of cyanuric chloride in 50 ml of hot dioxane was added to 50 ml of cold (0–5 °C), well stirred water, giving a white slurry.

* Author for correspondence.

0894–3230/93/010029–15$12.50

Received 22 April 1992
Revised 22 June 1992

A 16·15 g (163 mmol) amount of cyclohexylamine was added dropwise to the cold slurry, the mixture was allowed to warm to room temperature and 17·27 g of sodium carbonate were added slowly. The reaction mixture was then heated overnight at 80 °C with constant stirring. The resulting precipitate was filtered and washed with water to yield the product, m.p. 228–229 °C. Analysis: calculated for $C_{15}H_{24}N_5Cl$, C 58·15, H 7·81, N 22·60, Cl, 11·44; found, C 57·93, H 7·78, N 22·54, Cl 11·10%.

2,4,6-Tris(aminocyclohexyl)triazine (**1**). A 1 g (3.2 mmol) amount of 2,4-bis(aminocyclohexyl)-6-chlorotriazine was dissolved in 15 ml of hot dioxane. The hot solution was added to 15 ml of cold (0–5 °C) water while stirring. A 5 ml volume (43·7 mmol) of cyclohexylamine was added slowly and the mixture was heated at 80 °C for 48 h with stirring. The resulting precipitate was filtered and the white powder obtained was washed with water, m.p. 215–217 °C. Analysis: calculated for $C_{21}H_{36}N_6Cl$, C 67·70, H 9·74, N 22·56; found, C 67·40, H 9·45, N 22·30%.

2,4-Bis(aminocyclohexyl)-6-methoxytriazine (**2**). A mixture of 10 g (55·5 mmol) of 2,4-dichloro-6-methoxytriazine[11] and 150 ml of water was stirred vigorously at 0–10 °C while 21·78 g (220 mmol) of cyclohexylamine were added dropwise during 30 mins. The reaction was exothermic and a creamy yellow solution was obtained. An 11·7 g amount of sodium carbonate was added after the reaction mixture had been allowed to warm to room temperature. The resulting mixture was stirred and heated at 80 °C for 2 h. The creamy solution solidified and the product was filtered and washed with water. Two consecutive recrystallizations from heptane and methanol gave a white powder, m.p. 145–147 °C. Analysis: calculated for $C_{16}H_{27}N_5O$, C 62·91, H 8·92, N 22·94; found, C 62·94, H 8·70, N 22·78%.

2-Aminocyclohexyl-4,6-dichlorotriazine. A slurry of 5 g (27 mmol) of cyanuric chloride, 25 ml of dioxane and 20 ml water was prepared as described earlier, then 2·70 g (27 mmol) of cyclohexylamine were added dropwise while the mixture was kept below 5 °C. A 2·28 g amount of sodium hydrogencarbonate was added and the cooled solution was stirred for 1 h. The mixture was filtered and the resulting solid was washed with water. The product (3·4 g) was used without further purification in the preparation of 2-aminocyclohexyl-4,6-dimethoxytriazine (**7**).

2-Aminocyclohexyl-4,6-dimethoxytriazine (**7**). A 1·1 g amount of sodium hydroxide was dissolved in 50 ml of methanol, 3·4 g (13·8 mmol) 2-aminocyclohexyl-4,6-dichlorotriazine were added and the mixture was heated at 40 °C for 30 min and then at 75 °C overnight. On addition of water to the cooled solution, a white precipitate was obtained (2·45 g). The product was recrystallized from ethanol, m.p. 119 °C. Analysis: calculated for $C_{11}H_{18}N_4O_2$, C 55·45, H 7·61, N 23·51; found, C 54·89, H 7·75, N 22·43%.

Titrations. Typically, five to seven samples were prepared by introducing 0·033 mmol of host into each of the 4 mm NMR tubes. The guest was introduced into the tubes in different molar ratios, e.g. in the range 0·00825–0·0495 mmol. Approximately 400 μl of dry $CDCl_3$ were transferred into each of the tubes by a vacuum system and the tubes were then sealed with a flame. The volume of the solution was measured and host–guest concentrations were calculated.

RESULTS AND DISCUSSION

Conformational analysis of di- and triaminotriazines

2,4,6-Tris(aminocyclohexyl)triazine (**1**) is present in solution in two different conformations, **1a** and **1b**. At room temperature rapid exchange between the conformers occurs:

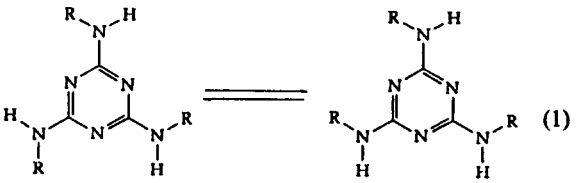

(1)

(1a) (1b)

Important parts of the ^1H and ^{13}C NMR spectra of **1** at room temperature (295 K) are shown in Figures 1(a) and 2(a), respectively. The ^1H NMR spectrum of **1** shows a broad-shouldered non-resolved signal at δ 4·65–4·90 ppm, corresponding to the different amine protons. The ^{13}C NMR spectrum reveals a singlet at δ 65·65 ppm for all aromatic carbons and a broad singlet at δ 49·13 ppm for the cyclohexyl carbon atoms adjacent to the amino groups. On cooling the $CDCl_3$ solution of **1**, slow exchange between the conformations is observed at 270 K, and the two conformations **1a** and **1b** are detectable in the ^1H and ^{13}C NMR spectra, Figures 1(b) and 2(b), respectively.

The ^1H NMR spectrum of **1** at 270 K reveals three doublets for the amine protons at δ 5·06, 4·99 and 4·92 ppm with an integration ratio corresponding to 1 : 1 : 4. In the ^{13}C NMR spectrum of **1** at 270 K the aromatic carbon atoms appear as four signals at δ 165·15, 164·82, 164·72 and 164·60 ppm and the cyclohexyl carbon atoms adjacent to amino triazine

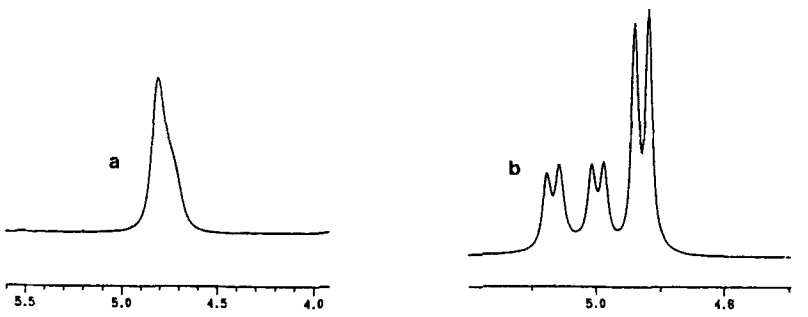

Figure 1. ^{1}H NMR spectrum of the amino protons of host **1** in $CDCl_3$ at (a) room temperature (295 K) and (b) 270 K

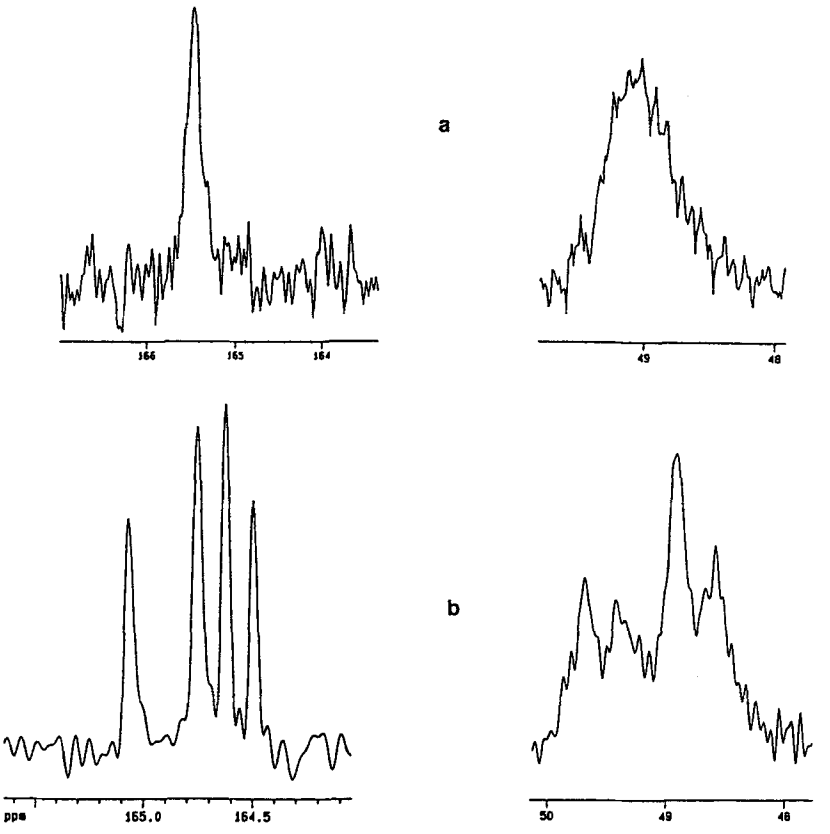

Figure 2. ^{13}C NMR spectrum of host **1** in $CDCl_3$ at (a) 295 K and (b) 270 K

groups appear at δ 49·66, 49·33, 48·88 and 48·50 ppm. As conformation **1a** exhibits C_3 symmetry whereas no symmetry element is present in conformation **1b**, we would expect that all amino protons and aromatic α-aminocyclohexyl carbons would reveal equivalency for conformation **1a**, whereas all amino protons and the respective carbon atoms should be non-equivalent in conformation **1b**. This would result in four distinct signals for the amino protons and aromatic and α-aminocyclohexyl carbon atoms on slow exchange between the conformations. Whereas the ^{13}C NMR spectrum at 270 K is consistent with this analysis, the ^{1}H NMR spectrum reveals only three doublets for the amino protons. As the theoretical integration ratio is

3 : 1 : 1 : 1 for conformations **1a** and **1b**, respectively, we realize that the integration ratio of the three doublets is 1 : 1 : 4, suggesting that two amino groups are isochronous. Within the temperature range examined, the cyclohexyl substituents are rapidly dynamically equilibrated and the α-aminocyclohexyl protons and carbons are averaged signals corresponding to axial and equatorial conformations.

We found that the coalescence temperature for the amine protons is $T_c = 280$ K. Hence the low limit exchange rate constant between the two conformations is $k_c = 24\ s^{-1}$, and the derived energy barrier for the conformational exchange corresponds to $\Delta G^{\#} = 14{\cdot}55 \pm 0{\cdot}2$ kcal mol^{-1} (1 kcal = 4·184 kJ).

Dynamic conformational analysis of a second triazine host, 2,6-bis(aminocyclohexyl)-4-methoxytriazine, (**2**), was similarly examined. At room temperature (295 K), **2** exists in three rapidly equilibrating conformations:

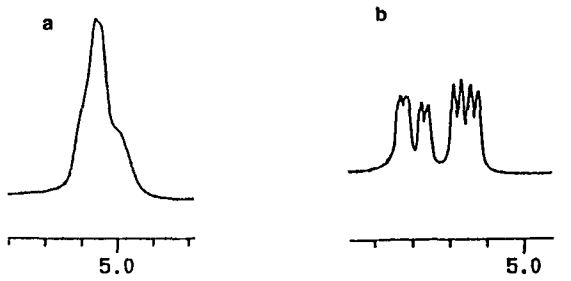

Figure 3. ^{1}H NMR spectrum of the amino protons of host **2** at (a) 295 K and (b) 270 K

The ^{1}H NMR spectrum ($CDCl_3$) of the amino protons is shown in Figure 3(a). It consists of a broad-shouldered signal in the region δ 4·85–5·03 ppm. Important bands in the ^{13}C NMR spectrum of **2** at 295 K

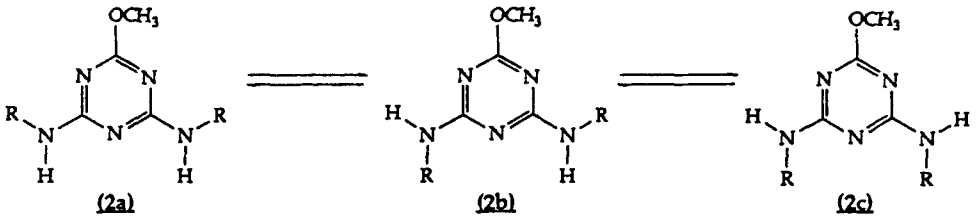

(2)

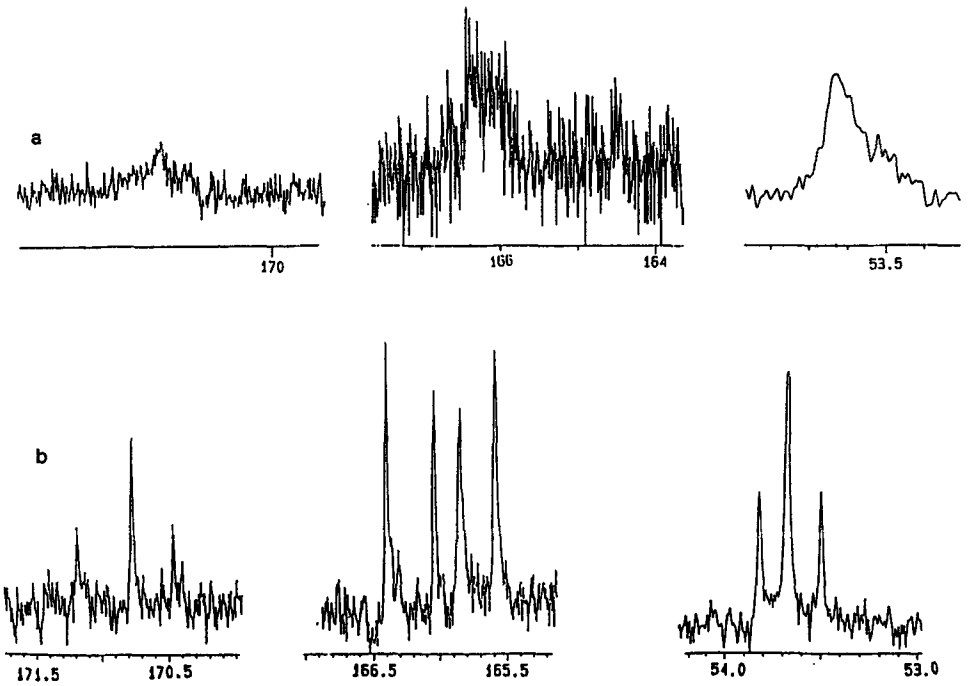

Figure 4. ^{13}C NMR spectrum of host **2** at (a) 295 K and (b) 270 K

[Figure 4(a)] include two bands at δ 166·24 and 171·63 ppm for the NH-linked aromatic carbons and CH_3O-linked aromatic carbons, respectively. The methoxy carbons of conformations **2a–c** appear as a single band at δ 53·43 ppm. Thus, at room temperature, rapid dynamic exchange between the three conformations takes place. On cooling the solution of **2** to 270 K, three distinct conformations, **2a–c**, are observed, implying that slow exchange among the conformations occurs. The ^{1}H NMR spectrum [Figure 3(b)] and ^{13}C bands [Figure 4(b)] reveal the existence of these three distinct conformations. The ^{1}H NMR bands of the amino protons appear as four separated doublets. As conformations **2a** and **2c** are symmetric whereas **2b** is asymmetric, four doublets are expected for the different conformations. The ^{13}C NMR bands confirm the existence of the three distinct conformations. The aromatic carbons are resolved into seven bands, where three bands of aromatic carbons adjacent to the methoxy group appear at δ 170·47, 170·77 and 171·78 ppm and four additional bands corresponding to the aromatic carbons linked to amino groups in the different conformations appear at δ 165·58, 165·89, 166·05 and 166·40 ppm. The methoxy carbon atoms are resolved into three bands at δ 53·50, 53·68 and 53·81 ppm. It should be noted that dynamic exchange of the methoxy group between *syn* and *anti* conformations and chair–chair cyclohexyl interconversion are still rapid at this temperature, and average conformations are observed for these processes.

The coalescence temperature for the dynamic exchange of conformations **2a–c** was followed for coalescence of the amino proton bands (T_c = 290 K) and for coalescence of the methoxy carbon atoms (T_c = 285 K). The derived energy barrier for the conformational exchange has been derived from the two coalescence temperatures to be $\Delta G^{\#}$ = 14·2 ± 0·2 and 14·5 ± 0·2 kcal mol^{-1}, respectively. As the amino proton also undergoes broadening on heating, the observed coalescence temperatures might be lower than the real values. Hence the derived energy barriers should be considered as low-limit values.

Conformational energy maps

Molecular mechanics (MM)[12a] calculations were performed on both compounds **1** and **2** using the MMX force-field method based on MM2 and MMPI programs developed by Allinger.[12b] Energy minimization of the molecules **1** and **2** results in structures in which all the nitrogen atoms of the amino groups are coplanar. This structure is in accordance with the previous x-ray single-crystal structure of 2,4,6-triamino-1,3,5-triazine.[13] The planarity of the amino groups in MM calculations arises from the effective conjugation of the amino nitrogen atoms with the π backbone. In contrast to aniline, where the amino nitrogen atoms show weak conjugation to the π system and thus only a poor correlation between MM calculations and experiments exists, here the nitrogen atoms exhibit a substantial aromatic character[14] and thus can be considered as π atoms. Therefore, MM calculations are expected to be a useful tool in predicting structural parameters of aminotriazine components.

Conformational energy maps of **1** and **2** were obtained by rotating the two dihedral angles θ and ϕ (Figure 5) in 10° increments and calculating the minimum potential energy for each set of angles. The conformational energy maps of **1** and **2** are shown in Figures 6 and 7, respectively.

For host **1**, only two minima are found [equation (1)], both having the same potential energy, implying that the two conformers are equally populated. The minima were found at $\theta = 0$, $\phi = 0$ (symmetric conformation) and $\theta = 180$, $\phi = 0$ (asymmetric conformation). The activation energy, E_a, for interconversion between these two stable conformations, was found to be 16 kcal mol^{-1}. These results are in accordance with dynamic NMR studies of host **1** that give a 1 : 1 ratio

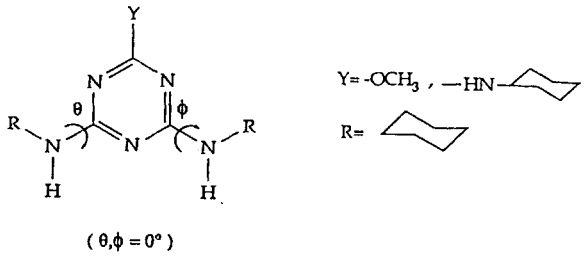

Figure 5. Schematic representation of the dihedral angles, θ and ϕ, in compounds **1** and **2**

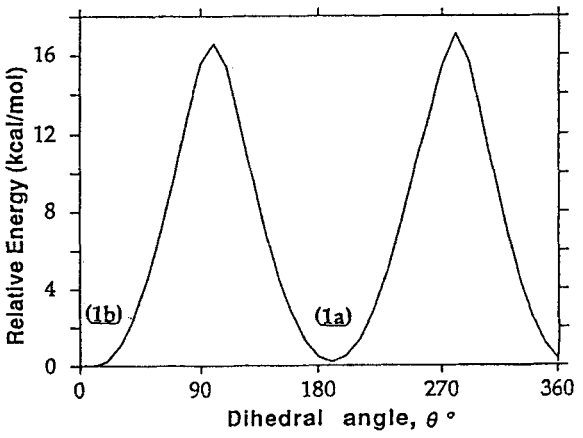

Figure 6. Potential energy profile of host **1** as a function of the torsional angle θ

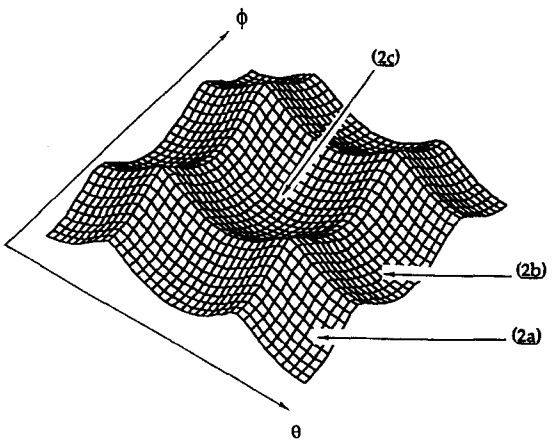

Figure 7. Conformational energy map of host **2** as a function of the torsional angles θ and ϕ

between the two conformers with an energy barrier of 14·55 kcal mol^{-1}.

For compound **2**, three minima are found [equation (2)]. The minima were found at $\theta = 0$, $\phi = 0$ (**2a**; symmetric conformation), $\theta = 180$, $\phi = 0$ (**2b**; asymmetric conformation) and $\theta = 180$, $\phi = 180$ (**2c**; antisymmetric conformation). The calculated **2a** : **2b** : **2c** conformational ratio is 1 : 1·75 : 2·43. The activation energies for isomerization, $E_{a(2a-2b)}$ and $E_{a(2b-2c)}$, were found to be 16·88 and 17·26 kcal mol^{-1}, respectively. NMR studies of host **2** indicated a 1 : 1 : 3 population ratio of the three conformers. We assume that the most stable conformer is **2c**, as found in the MMX calculations.

Design of H-bonded host–guest interactions between 1 or 2 and 1,3-keto functionalities – a molecular mechanics approach

Hydrogen-bonded assemblies[15] involve the participation of at least three types of interaction mechanisms, that is, electrostatic, dispersive and charge-transfer interactions. In the last few years, the dominant role of coulombic interactions (electrostatic interactions) has become apparent through quantum-chemical calculations. As MM calculations treat H-bonds as electrostatic interactions,[12] we applied the MM method for predicting and designing H-bonded assemblies between **1** and **2** simulation of host–guest assemblies.

The binding ability of hosts **1** and **2** towards 1,3-diketones, i.e. bemegride (**3**), was studied using the MMX program. For 2,4,6-tris(aminocyclohexyl)triazine (**1**) each of the stable conformers (**1a** and **1b**) was interacted with **3** and the energy of the resulting bimolecular assembly was minimized. In fact, for the purpose of calculations, the 1,3-diketone **3** was forced to short distance (*ca* 2·5 Å) from the conformations **1a** and **1b** [see equation (3)]. The energy of the resulting assembly was minimized until a structure of minimum potential energy was obtained.

For the symmetric conformation **1b** a stable three H-bonded assembly is formed. The calculated structural parameters of this assembly and its bimolecular configuration are shown in Figure 8. The calculated enthalpy change associated with the formation of this assembly corresponds to $\Delta H = -16{\cdot}21$ kcal mol^{-1}. On the other hand, where a similar computational analysis is performed for the asymmetric conformation **1a**, the two components separate from one another and no bimolecular H-bonded assembly of minimum potential energy is formed.

When both components are placed in an orthogonal position with respect to one another and minimization is performed, the complex dissociates and thus the linear configuration of the assembly represents a global minimum on the potential energy surface of the complex.

The same procedure was applied for association of the three stable conformations of **2** with **3**. Here we find that conformation **2a** yields a stable three H-bonded assembly of minimum potential energy **2a**–**3**, exhibiting the calculated structural parameters shown in Figure 9. The other two conformations (**2b** and **2c**) separate from

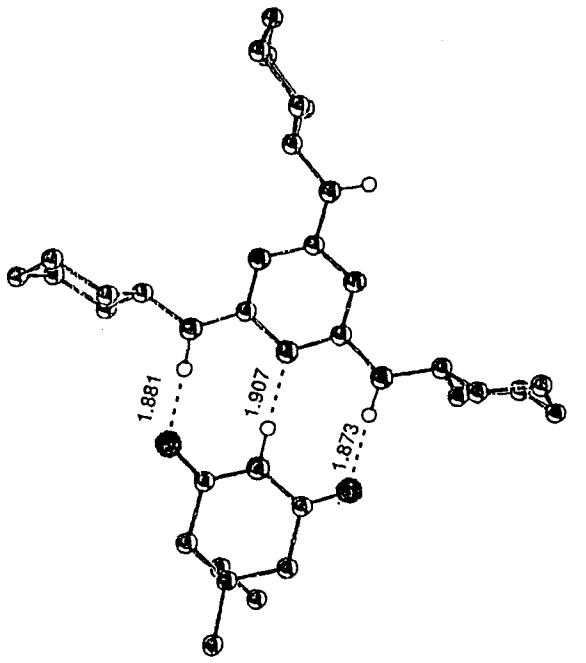

Figure 8. Calculated minimum energy structure of the complex **1b**–**3**

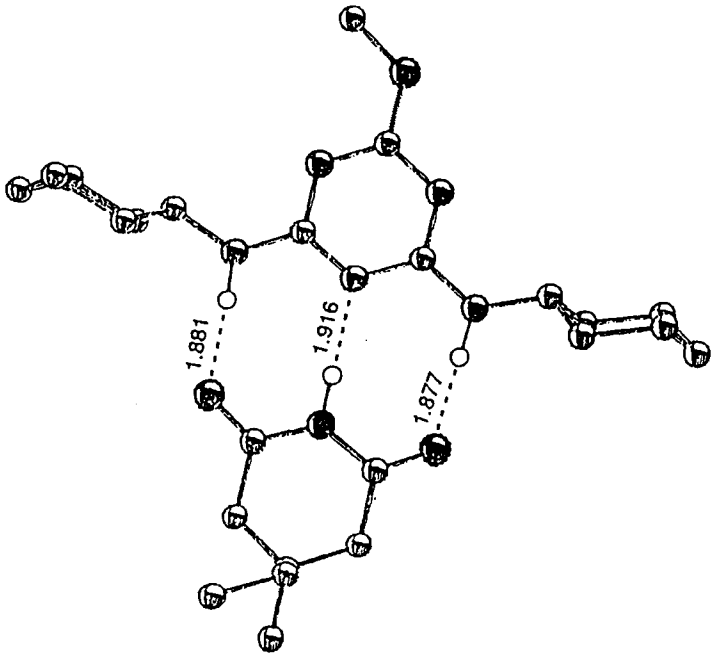

Figure 9. Calculated minimum energy structure of the complex **2a**–**3**

3 within the energy minimization process, implying that the latter conformations are not stabilized by complementary H-bonded interactions. The enthalpy change associated with the formation of **2a**–**3** is $\Delta H = -15{\cdot}93$ kcal mol^{-1}.

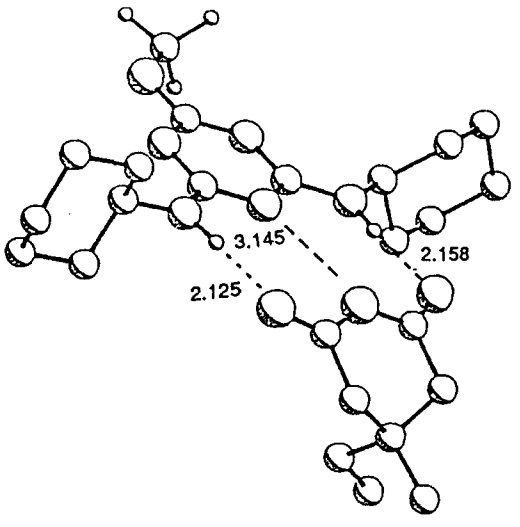

Figure 10. Calculated minimum energy structure of the complex **2a**–**4**

Molecular mechanics calculations were also performed on the association of 3-ethyl-3-methylglutaric anhydride (**4**) with **2**. With **4** only two complementary H-bonds to **2** are possible. Simulation of the association process yields a stable H-bonded assembly between **4** and conformation **2a** of the triazine component. Interestingly, the anhydride moiety is not coplanar with the triazine complementary unit and the oxygen atom comprising the anhydride ring is tilted by *ca* 22° relative to the triazine plane (Figure 10). This non-planar structure might be attributed to electrostatic repulsive interactions between the triazine sp^2 nitrogen atom and the anhydride oxygen atom. The calculated enthalpy change associated with the formation of **2a**–**4** corresponds to $\Delta H = -8{\cdot}6$ kcal mol^{-1}. Hence the lower value of the enthalpy change in the assembly **2a**–**4** as compared with the value of **2a**–**3** suggests a lower association constant for the structure **2a**–**4**. This lower association constant might be attributed to the stabilizing effect of two H-bonds only and the destabilization effect of intermolecular repulsive electrostatic interactions.

H-bonded assemblies using aminotriazine hosts

According to the calculations, we find that the association of bemegride (**3**) with **1** and **2** proceeds by discrimination of the theoretically predicted conformation of the triazine molecules. The complexation processes

were studied and followed by means of NMR. Figure 11 shows the spectral changes in the ^{1}H NMR spectrum of **1** that occur on increasing the concentration of **3**. It is evident that the amino protons of **1** appearing as a broad signal at δ 4·65–4·90 ppm are split into two bands on addition of **3**. One band, corresponding to H_a and $H_{a'}$ in conformation **1b**–**3** [see equation (3)] is shifted downfield as the concentration of **3** is increased, whereas the second amino band, corresponding to H_b and all amino groups in both free conformations **1a** and **1b**, is not shifted. The integration ratio of the shifted band and fixed band is, however, affected by the concentration of **3**, and the shifted band increases progressively in its intensity relative to the fixed band on addition of **3**. At high concentrations of **3**, the integration ratio between the shifted band and fixed NMR amino signal corresponds to 2 : 1. These results suggest that association of **3** with **1** proceeds by complementary H-bonded interactions: the amino protons being shifted downfield participate in intermolecular H-bond formation whereas the amino proton in the fixed position is free from such interactions. The integration ratio of the two bands at high concentrations of **3** implies the two amino protons participate in the H-bond interactions whereas the third amino group is non-interactive. These results are consistent with the formation of a three-site H-bonded assembly between bemegride and conformation **1b** [equation (3)], that is, only conformation **1b** is capable of generating three anchoring sites for H-bonds with **3**:

The ^{13}C NMR spectrum of the resulting H-bonded assembly is consistent with the intermolecular structure **1b**–**3**. Figure 12 shows important ^{13}C NMR bands of the resulting assembly in a sample consisting of **1** and **3** in a 1 : 1 ratio (295 K). Only three ^{13}C NMR bands for the triazine aromatic carbon are detectable at δ 164·50, 164·67 and 164·83 ppm and two α-aminocyclohexyl carbon atoms at δ 48·64 and 49·47 ppm. Any two-site association of **3** with **1a** or a non-selective association of **3** with the conformers **1a** and **1b** would result in a more complex ^{13}C NMR spectrum.

Further support for the formation of the intermolecular complex **1b**–**3** is obtained from NOE NMR studies. Figure 13 shows the ^{1}H NMR NOESY spectrum of a solution consisting of **1** and **3** in a molar ratio of 1 : 1. Three cross-peaks are observed: one is obtained between the H-bonded protons H_a, $H_{a'}$ and the free amino proton H_b, the second between H_a, $H_{a'}$ and H_c and the third between H_b and H_c. The 1D-ROESY spectrum using a shaped pulse to excite H_c yields through-space correlations (negative) with H_a and $H_{a'}$ only. Hence the correlation of H_c with H_b and of H_a, $H_{a'}$ to H_b observed in the 2D-NOESY spectrum probably arises from spin diffusion or exchange. Of particular interest are the correlations between H_a, $H_{a'}$ and H_c observed in the NOESY and ROESY spectra. This implies that the respective amino protons of the two counter-components **1** and **3** are in close spatial arrangement, exhibiting mutual magnetic through-space interactions, as ascribed in structure **1b**–**3**.

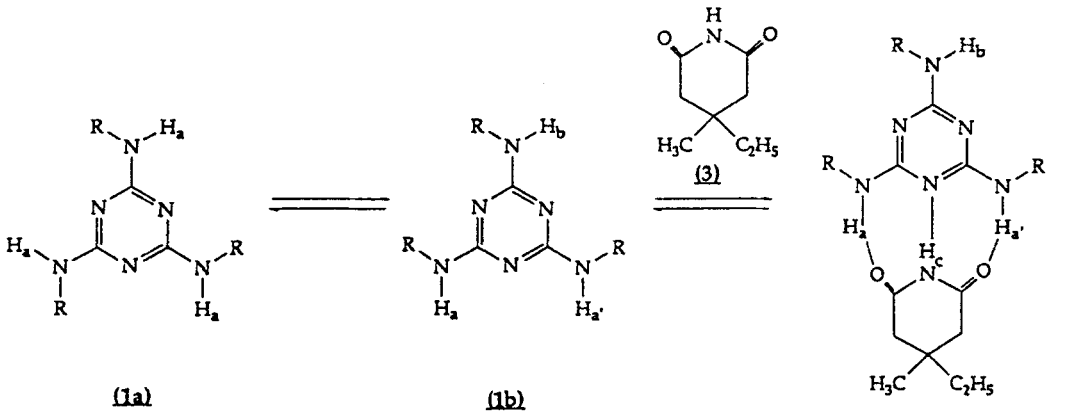

(3)

On addition of **3**, only conformation **1b** is recognized by **3** to form the intermolecular complex (**1b**–**3**). As a result, the conformation equilibrium between **1a** and **1b** is affected by added **3**, and is constantly shifted towards the conformation stabilized in the complex structure. At high concentrations of **3**, the triazine host is almost entirely in the complex structure and exhibits the conformation **1b**. Under these conditions the integration ratio of bound and free amino protons indeed corresponds to 2 : 1.

From the downfield shifts of the amino protons of **1** at different concentrations of **3** the association constant for formation of the H-bonded assembly is found to be $K_a = 915\ \mathrm{l\,mol^{-1}}$.

Another aspect to consider is the effect of formation of the H-bonded assembly **1b**–**3** on the conformational equilibrium between **1a** and **1b**. As discussed earlier, conformations **1a** and **1b** are rapidly equilibrating at room temperature, although the coalescence temperature is close to room temperature. On addition

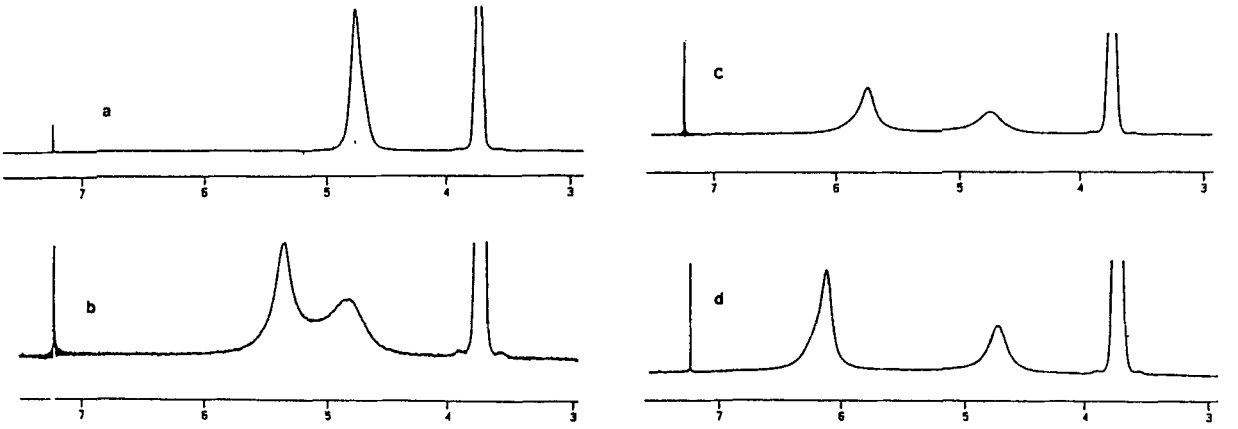

Figure 11. ^{1}H NMR spectra of **1**, 0·074 M in $CDCl_3$, in the presence of **3**. Concentrations of **3**: (a) 0; (b) 0·02; (c) 0·047; (d) 0·074 M

of **3** (at low concentration) to a solution of **1** [Figure 11(b)], formation of the intermolecular H-bonded assembly **1b**–**3** decreases the population of free conformers **1a** and **1b**. As a result, the **1a** ⇌ **1b** conformational exchange rate is slower and the amine protons of the two conformations are resolved at 315 K (implying slow exchange). To effect rapid exchange between **1a** and **1b** in the presence of added **3**, slight heating of the sample is required. Accordingly, the barrier for rapid **1a** ⇌ **1b** interconversion will depend on the concentration of added **3**. Indeed, we find that a host–guest molar ratio of 2 : 1 and 1 : 1 results in slow exchange between conformers **1a** and **1b** at room temperature, and the low-limit energy barrier for rapid **1a** ⇌ **1b** interconversion corresponds to $\Delta G^{\#} = 14{\cdot}77$ and 15·03 kcal mol^{-1} at these two ratios, respectively.

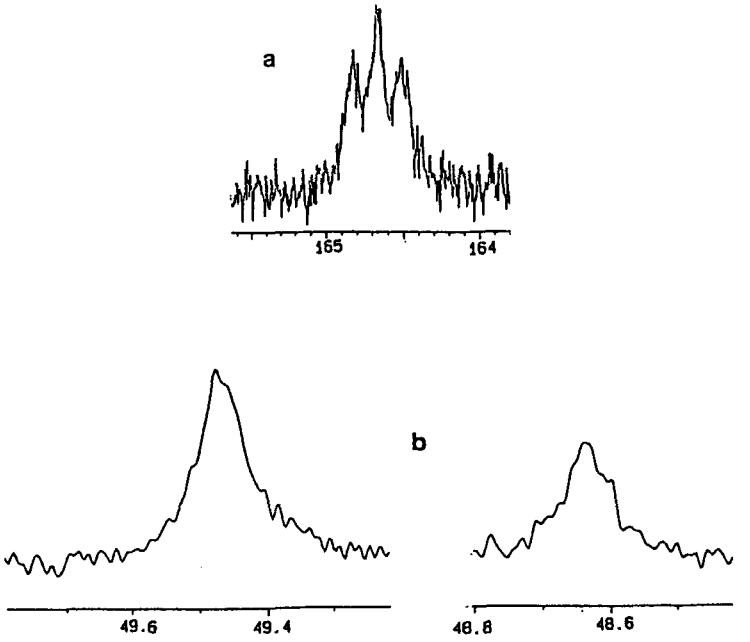

Figure 12. ^{13}C NMR spectra of a $CDCl_3$ solution of **1** and **3** in a 1 : 1 molar ratio at 295 K. (a) Aromatic carbons; (b) α-aminocyclohexyl carbons

Similarly, association of **2** with bemegride (**3**) involves selective recognition of conformation **2a** for formation of the H-bonded intermolecular assembly **2a–3**:

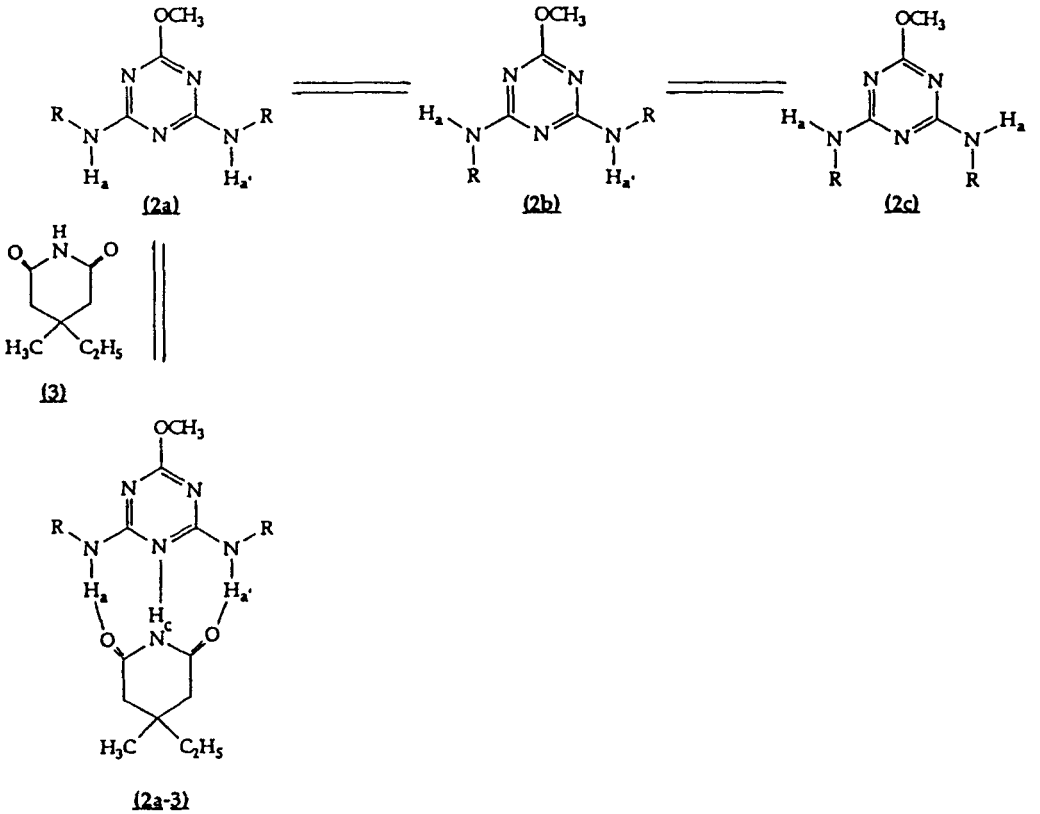

(4)

The conformational selectivity is predicted by molecular mechanics calculations.

Addition of **3** to a dry $CDCl_3$ solution of **2** results in the ^1H NMR spectra shown in Figure 14. The amine protons of **2**, appearing as a broad band at δ 4·99–5·15 ppm in the absence of **3**, are split into three bands on addition of **3**. One band, corresponding to protons H_a and $H_{a'}$ in conformation **2a–3** [equation (4)], is shifted downfield on increasing the concentration of **3**, whereas the other two bands which represent the amino protons in conformations **2b** and **2c** appear at constant chemical shifts, δ 5·11 and 4·94 ppm. The intensities of the bands later decrease on addition of **3** and at high **3** concentrations (0·17 M) the two bands almost disappear [Figure 14(d)]. The downfield-shifted protons appear at a constant chemical shift, δ 6·95 ppm, at high concentrations of **3**.

Figure 15 shows the titration curve corresponding to the NMR shifts of **2** on addition of **3** (at 270 K). Evidently, only one set of amino-protons (H_a and $H_{a'}$) are shifted and reach a saturation value on complete complexation. Hence the ^1H NMR spectra reveal that on addition of **3** slow exchange between the conformers is induced and the amino proton bands of conformers **2a–c** are resolved. In addition, amino protons of one conformer (H_a and $H_{a'}$) participate in the generation of an H-bonded assembly and these protons are shifted downfield, whereas the other two conformations do not participate in such intermolecular association. Further, stabilization of the specific conformer in the form of an H-bonded assembly shifts the conformational equilibrium, on addition of **3**, to the favoured conformer recognized by **3**. Insight into the selected conformation recognized by **3** and the structure of the resulting H-bonded intermolecular complex is obtained from ^{13}C and ^1H NMR NOE measurements. ^{13}C NMR studies were performed on a sample including **2** and **3** in a 1 : 1 molar ratio. Under these conditions **2** is almost entirely in the H-bonded associated assembly. Important ^{13}C bands of the resulting complex are

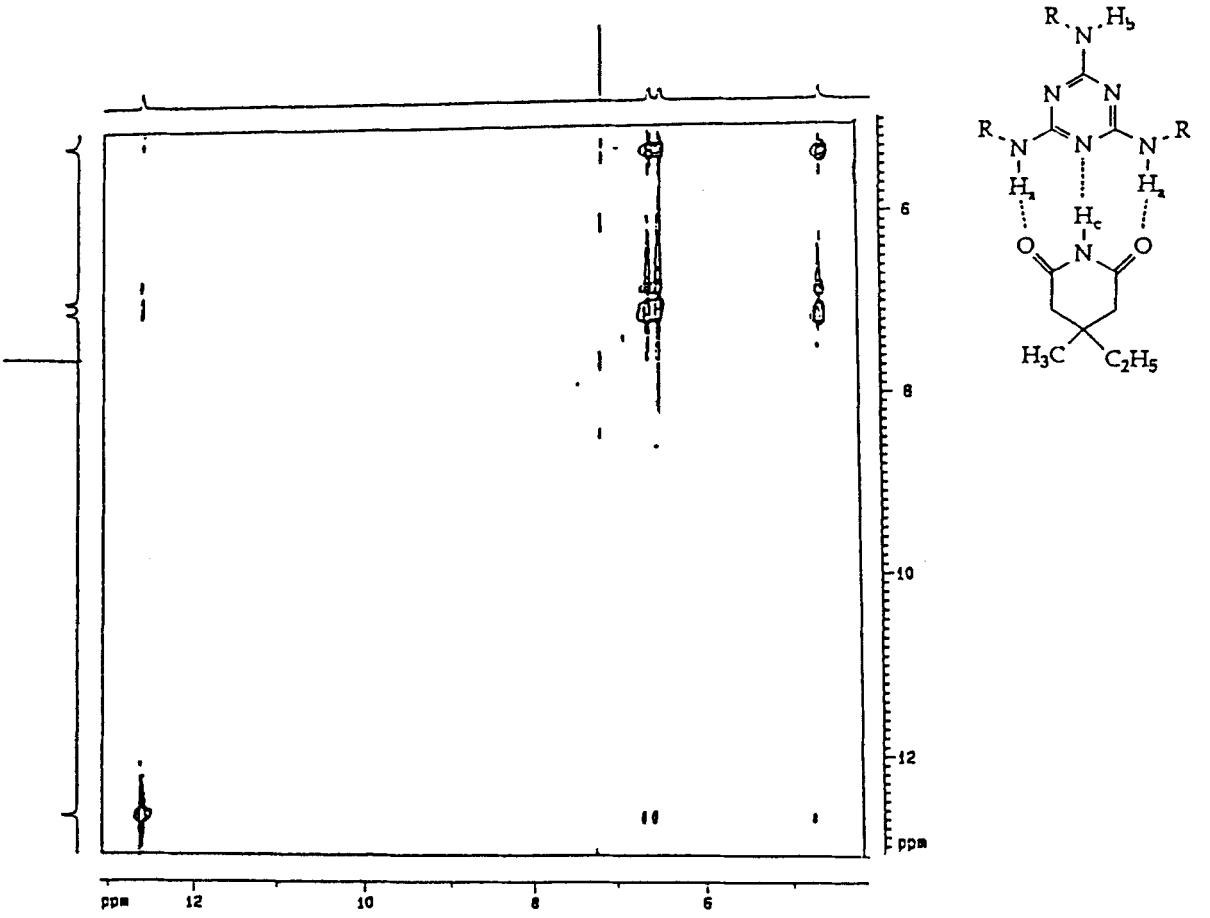

Figure 13. NOESY spectrum of a $CDCl_3$ spectrum of **1** and **3** in a 1 : 1 molar ratio at 250 K

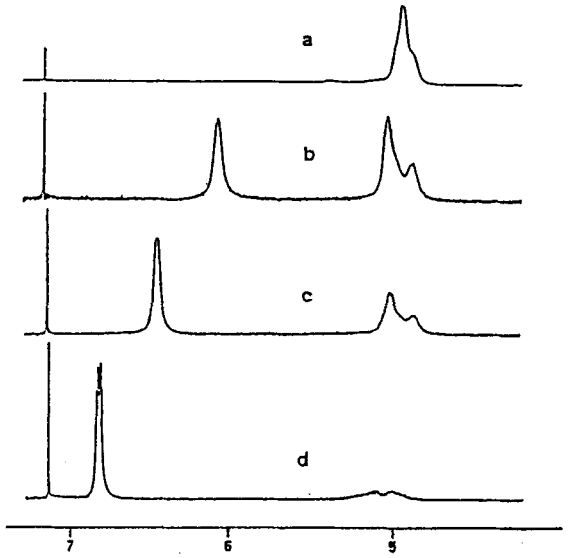

Figure 14. ^1H NMR spectra of **2**, 0·082 M, in the presence of **3**. Concentrations of **3**: (a) 0; (b) 0·024; (c) 0·049; (d) 0·017 M

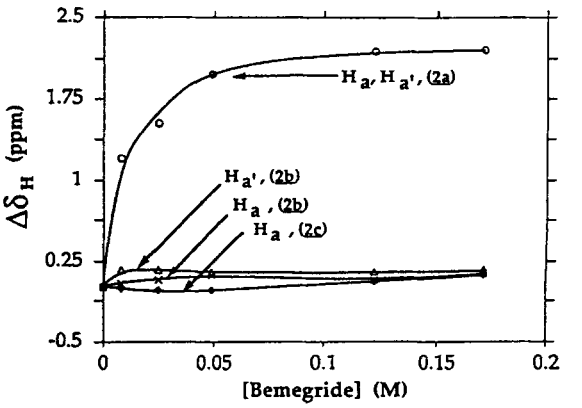

Figure 15. Titration curve of host **2** on addition of **3** at 270 K

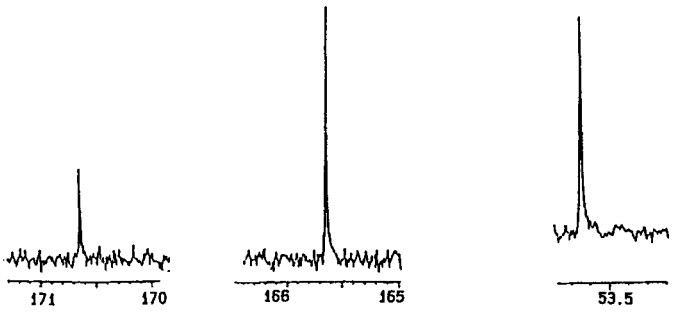

Figure 16. ^{13}C NMR spectrum of the complex **2**–**3** at 270 K

shown in Figure 16 (270 K). It is evident that only one carbon band of the $-OCH_3$ group is observed at 53·64 ppm and two carbon bands are observed in the aromatic region. The later bands correspond to the aromatic carbon adjacent to the methoxy group, δ 170·69 ppm, and the aromatic carbon linked to the amino groups, δ 165·64 ppm. This simple ^{13}C NMR spectrum formed in the presence of **3** (270 K), when compared with the previously discussed ^{13}C NMR spectrum of **2** [Figure 4(b)], consisting of the three resolved conformations **2a**–**c**, reconfirms that at a 1 : 1 molar ratio of **2** and **3** an intermolecular H-bonded complex

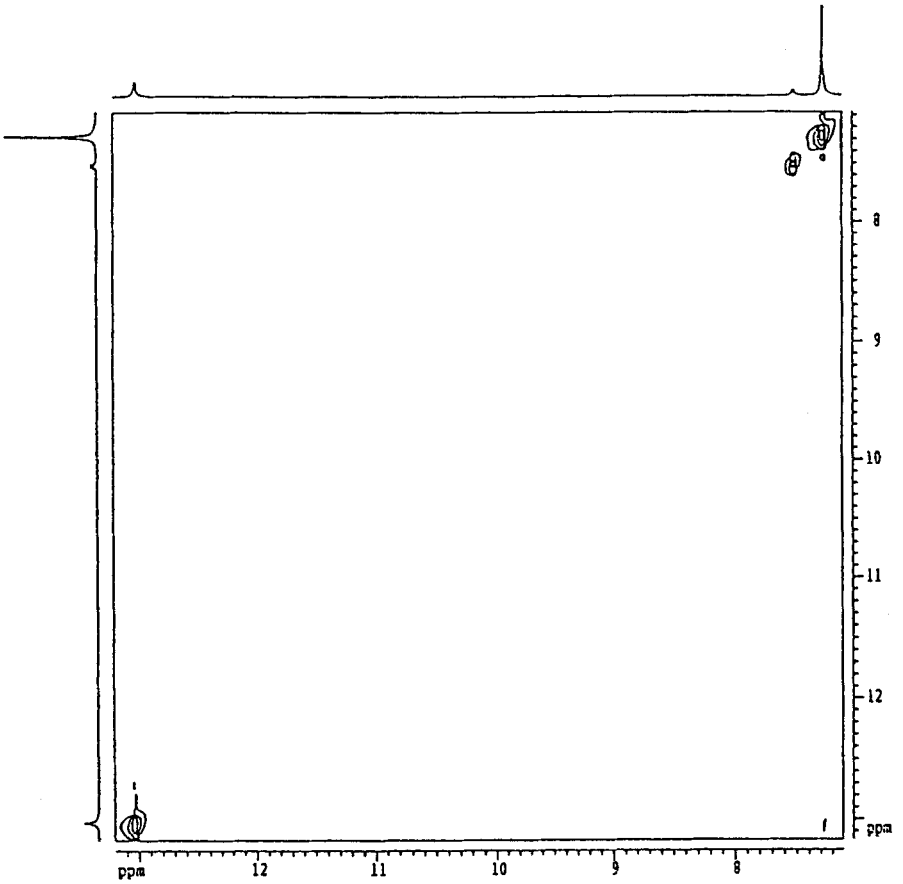

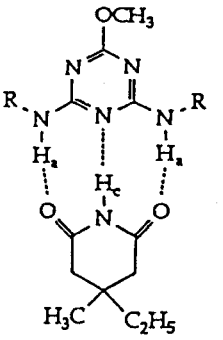

Figure 17. NOESY spectrum of a $CDCl_3$ solution containing **2** and **3** in a 1 : 1 molar ratio at 220 K

is formed with a favoured conformation of **2**. The stability of this complex pulls the equilibrium of the conformers to the selected conformational structure generating the H-bonded assembly. As the ^{13}C NMR spectrum of the complex reveals C_{2v} symmetry of the assembly (equivalence of carbon atoms linked to amine groups), conformation **2b** can be excluded as the selected recognized conformation. Similarly, the molecular mechanics calculations discussed earlier implied that the hydrogen atoms in **2c** are too far apart to generate complementary H-bonds with **3**, whereas conformation **2a** exhibits the proper structure for such a 'three-point' interaction. We therefore conclude that **3** recognizes and selects conformation **2a** in assembling the intermolecular H-bonded complex **2a–3** [equation (4)]. Further support for the formation of this complex is obtained from ^1H NMR NOE experiments (Figure 17). It is evident that a cross-peak between the amino protons of **2a**, H_a (δ 7·28), and the amine proton of **3**, H_c (δ 13·05 ppm), is obtained, implying that intermolecular magnetic interactions are operative as a result of close association.

From the downfield shifts of amino protons of **1** at different concentrations of **3**, the association constant for the complex **2a–3** is derived and exhibits the value $K_a = 450\ l\,mol^{-1}$.

A further aspect to discuss involves the relative association constants of the assemblies **1b–3** and **2a–3**, which include three complementary H-bonded interactions and a comparison of the association constant of our systems with those of other 'three-point' H-bonded assemblies. We realize that the association constant of **1b–3** is higher than that of **2a–3** by a factor of two. This might be attributed to an entropic effect associated with the selective binding of **3** to the amino triazines: whereas **1** is present in two conformations [equation (3)], the host molecule **2** is present in three conformations, [equation (4)]. Hence discrimination of the conformer **2a** for selective association of **3** is accompanied by a larger entropic loss as compared with the discrimination of **1b** out of two conformations. This is reflected in the lower association constant of **2a–3**.

Comparison of the association constants of **1b–3** and **2c–3** with other 'three-point' H-bonded assemblies is also interesting. Scheme 1 shows the association modes of two 'three-point' H-bonded assemblies including the system in this study. We realize that the association constants of the assemblies studied here are lower by almost two orders of magnitude than those of the guanine–cytosine base pair (**5–6**).[16] In a recent theoretical account by Pranata *et al.*,[5] the factors controlling the association properties of 'three-point' H-bonded assemblies were considered. It was emphasized that not only is the stability of these assemblies controlled by the primary H-bond interactions, but also secondary electrostatic interaction of adjacent H-bonding sites play important roles in the bimolecular association process. As the H atom and electronegative atom participating in the bond formation can be considered as an electron-donor and -acceptor site, respectively, three different association patterns of three H-bonded assemblies are feasible (Scheme 2). In configuration (a) three repulsive and two attractive electrostatic interactions are present. In configuration (c) all primary H-bonds are accompanied by four secondary attractive interactions and these assemblies represent the most stable three H-bonded assemblies. The complexes **1b–3** and **2a–3** represent H-bonded assemblies where electron-donor and -acceptor sites alternate in both components of the assembly (Scheme 2) [analogous to configuration

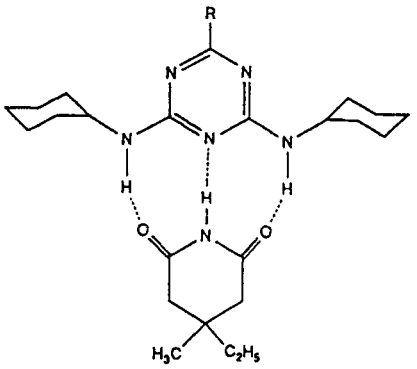

(1b)-(3) , R= NH- , K= 915 M^{-1}

(2a)-(3) , R= -OCH_3 , K= 450 M^{-1}

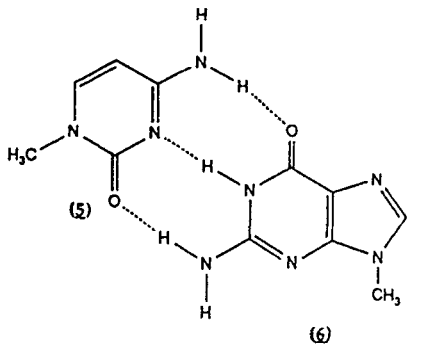

(5)-(6), K= 10^4-10^5 M^{-1}

Scheme 1. Proposed secondary interactions in 'three-point' H-bonded assemblies

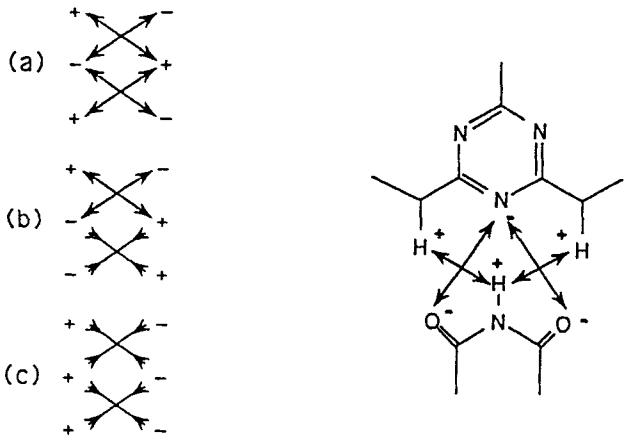

Scheme 2. Schematic representation of the association patterns of a 'three-point' H-bonded assembly

(a)]. Our molecular mechanics calculations revealed that the distances between the electrostatic sites of adjacent H-bonds are in the range 2·4–3·6 Å. Hence the mutual repulsive interactions destabilize the intermolecular complex. On the other hand, the base pair **5**–**6** represents configuration (b), where the repulsive interactions are compensated by a pair of attractive interactions. As a result, this complex exhibits higher stabilization than **1b**–**3** and **2a**–**3**, as reflected by its association constant.

In this respect, it should be noted that 2-aminocyclohexyl-4,6-dimethoxytriazine (**7**) exhibits very weak association with **3**, $K_a = 16\,l\,mol^{-1}$. This weak association constant might be attributed to the presence of only two anchoring sites in **7** and to the destabilization of the complex by electrostatic repulsion between the carbonyl oxygen and the methoxy group. Similarly, we find that the association constant of 3-ethyl-3-methylglutaric anhydride (**4**) with **2** exhibits an association constant of $K_a = 10\,l\,mol^{-1}$. This assembly includes only 'two-point' H-bonds but destabilizing electrostatic repulsions between the anhydride oxygen interactions were reflected in the molecular mechanics calculations by distortion of the anhydride ring from the triazine plane by *ca* 22° (see above). Hence the low value of the association constant of **2a**–**4** originates from lower intermolecular H-bonds and intermolecular electrostatic repulsive interactions.

CONCLUSIONS

We have studied the conformational behaviour of diamino- and triaminotriazines and correlated molecular mechanics calculations with the experimental conformational dynamics of these compounds. We have also followed the formation of H-bonded assemblies between **1**, **2** and the complementary host molecular bemegride (**3**). We find that the formation of the 'three-point' H-bonded intermolecular complexes proceeds by selection of a discrete conformation of the triazine hosts to form **1b**–**3** and **2a**–**3** H-bonded complexes. The intermolecular association process is controlled by primary intermolecular H-bonds and influenced by secondary electrostatic repulsive interactions of adjacent H-bonding sites.

ACKNOWLEDGEMENT

The assistance of Dr R. E. Hoffman in the NOESY and ROESY NMR experiment is gratefully acknowledged.

REFERENCES

1. (a) H. Kessler, *Angew. Chem., Int. Ed. Engl.* **21**, 512–523 (1982); (b) R. J. P. Williams, *Angew. Chem. Int. Ed. Engl.* **16**, 766–777 (1977).
2. (a) F. Garcia-Tellado, S. Goswami, S.-K. Chang, S. J. Geib and A. D. Hamilton, *J. Am. Chem. Soc.* **112**, 7393–7394 (1990); (b) P. Tecilla, R. P. Dixon, G. Solobodkin, D. S. Alalvi, D. H. Waldeck and A. D. Hamilton, *J. Am. Chem. Soc.* **112**, 9408–9410 (1990); (c) Y. Tanaka, Y. Kato and Y. Aoyama, *J. Am. Chem Soc.* **112**, 2807–2808 (1990); (d) S.-K. Chang, D. Van Engen, E. Fan and A. D. Hamilton, *J. Am. Chem. Soc.* **113**, 7640–7645 (1991).
3. (a) M. Tamulok, K. S. Jeong, G. Deslongchamps and J. Rebek, Jr, *Angew. Chem., Int. Ed. Engl.* **30**, 858–859 (1991); (b) K. M. Neder and H. W. Whitlock, Jr, *J. Am. Chem. Soc.* **112**, 9412–9414 (1990); (c) K. S. Jeong, T. Tjivikua, A. Muehldorf, D. Deslongchamps, N. Famulok and J. Rebek, Jr, *J. Am. Chem. Soc.* **113**, 201–209 (1991); (d) J. Rebek, Jr, *Acc. Chem. Res.* **23**, 399–404 (1990); (e) T. Benzing, T. Tjivikua, J. Wolfe and J. Rebek, Jr, *Science* **242**, 266–268 (1988).
4. (a) W. L. Jorgensen and D. L. Severance, *J. Am. Chem. Soc.* **113**, 209–216 (1991); (b) J. S. Lindsey, *New J. Chem.* **15**, 153–180 (1991); (c) J. Rebek, Jr, *J. Am. Chem. Soc.* **109**, 2426–2431 (1987); (d) J. Rebek, Jr, *Science* **235**, 1478–1484 (1987).
5. J. Pranata, S. G. Wierschke and W. L. Jorgensen, *J. Am. Chem. Soc.* **113**, 2810–2819 (1991).
6. C. Vincent, S. C. Hirst, F. Garcia-Tellado and A. D. Hamilton, *J. Am. Chem. Soc.* **113**, 5466–5467 (1991).
7. (a) C. T. Seto and G. M. Whitesides, *J. Am. Chem. Soc.* **112**, 6409–6411 (1990); (b) C. T. Seto and G. M. Whitesides, *J. Am. Chem. Soc.* **113**, 712–713 (1991).
8. K. Kurihama, K. Ohto, Y. Honda and T. Kunitake, *J. Am. Chem. Soc.* **113**, 5077–5079 (1991).
9. M. D. Joesten and L. J. Schaad, *Hydrogen Bonding*, pp. 173–175. Marcel Dekker, New York (1974).
10. J. T. Thurston, J. R. Dudley, D. W. Kaiser, I. Hechenbleikner, F. C. Schaefer and D. Holm-Hansen, *J. Am. Chem. Soc.* **73**, 2981–2983 (1951); (b) D. W. Kaiser, J. T. Thurston, J. R. Dudley, F. C. Schaefer, I. Hechenbleikner and D. Holm-Hansen, *J. Am. Chem. Soc.* **73**, 2984–2986 (1951).

11. J. R. Dudley, J. T. Thurston, F. C. Schaefer, D. Holm-Hansen, C. J. Hull and P. Adams, *J. Am. Chem. Soc.* **73**, 2986–2990 (1951).
12. (a) PCMPI Ver. 4.2 program, formerly PCMODEL-PI, Serena Software, Bloomington, IN; (b) N. L. Allinger, *J. Am. Chem. Soc.* **99**, 8127–8134 (1977).
13. J. N. Vareghese, A. M. O'Connell and E. N. Maslen, *Acta Crystallogr., Sect. B* **33**, 2102–2108 (1977).
14. (a) C. Grundmann, L. Schwennicke and E. Beyer, *Chem. Ber.* **87**, 19–24 (1954); (b) W. Weith, *Chem. Ber.* **9**, 454–463 (1876); (c) A. Claus, *Chem. Ber.* **9**, 721–724 (1876).
15. H.-J. Schneider, *Angew. Chem., Int. Ed. Engl.* **30**, 1417–1436 (1991).
16. (a) Y. Kyogoku, R. C. Lord and A. Rich, *Biochim. Biophys. Acta* **179**, 10–17 (1969); (b) T. R. Kelly, C. Zhao and G. J. Bridges, *J. Am. Chem. Soc.* **111**, 3744–3745 (1989).